atmosphere

MDPI

Article

Analysis of Spatial and Temporal Variations of the Near-Surface Wind Regime and Their Influencing Factors in the Badain Jaran Desert, China

Ziying Hu [1,2,3], Guangpeng Wang [1,2,3], Yong Liu [4], Peijun Shi [1,2,3], Guoming Zhang [1,2,3], Jifu Liu [1,2,3], Yu Gu [1,2,3], Xichen Huang [1,2,3], Qingyan Zhang [1,2,3], Xu Han [1,2,3], Xueling Wang [1,2,3], Jiewen Du [1,2,3], Ruoxin Li [1,2,3] and Lianyou Liu [1,2,3,*]

1 Key Laboratory of Environmental Change and Natural Disaster, Ministry of Education, Beijing Normal University, Beijing 100875, China
2 Engineering Research Center of Desertification and Blown-Sand Control, Ministry of Education, Beijing Normal University, Beijing 100875, China
3 Academy of Disaster Risk Science, Faculty of Geographical Science, Beijing Normal University, Beijing 100875, China
4 National Institute of Natural Hazards, Ministry of Emergency Management of China, Beijing 100085, China
* Correspondence: lyliu@bnu.edu.cn

Abstract: Wind regime is one of the main natural factors controlling the evolution and distribution of aeolian sand landforms, and sand drift potential (DP) is usually used to study the capacity of aeolian sand transport. The Badain Jaran Desert (BJD) is located where polar cold air frequently enters China. Based on wind data of eight nearby meteorological stations, this research is intended to explore the temporal variation and spatial distribution features of wind speed and DP using linear regression and cumulative anomaly method, and reveal the relationship between atmospheric circulation and wind speed with correlation analysis. We found that the wind speed and frequency of sand-blowing wind in the BJD decreased significantly during 1971–2016, and the wind speed obviously mutated in 1987. The regional wind speed change was affected by the Asian polar vortex, the northern hemisphere polar vortex and the Tibet Plateau circulation. The wind rose of the annual sand-blowing wind in this region was the "acute bimodal" type. Most of the annual wind directions clustered into the W-NW, and the prevailing wind direction was WNW. During 1971–2016, the annual DP, the resultant drift potential (RDP) and the directional variability (PDP/DP) in the desert showed an obvious downtrend, with a "cliff-like" decline in the 1980s and relative stable fluctuation thereafter. The BJD was under a low-energy wind environment with the acute bimodal wind regime. Wind speed, sand-blowing wind frequency and DP were high in the northeast and low in the southwest.

Keywords: wind regime; sand-blowing wind; sand drift potential; atmospheric circulation; Badain Jaran Desert

check for updates

Citation: Hu, Z.; Wang, G.; Liu, Y.; Shi, P.; Zhang, G.; Liu, J.; Gu, Y.; Huang, X.; Zhang, Q.; Han, X.; et al. Analysis of Spatial and Temporal Variations of the Near-Surface Wind Regime and Their Influencing Factors in the Badain Jaran Desert, China. *Atmosphere* **2022**, *13*, 1316. https://doi.org/10.3390/atmos13081316

Academic Editors: Wei Shi, Qihu Sheng, Fengmei Jing, Dahai Zhang and Puyang Zhang

Received: 27 June 2022
Accepted: 13 August 2022
Published: 18 August 2022

1. Introduction

In general, wind serves as one of the main driving forces in shaping landforms, especially in arid and semi-arid regions [1–4]. As a vector, wind has both wind speed and direction that control the magnitude and orientation of sand transport, respectively. International studies on typical dunes in sand seas indicated the close relationship between regional wind regimes and dune types [5–7]. As a clean and renewable resource, wind energy can be used for wind power generation, but it can also bring adverse effects, such as wind-sand electromagnetic disturbance and desertification expansion [8–10]. Over the past decades, wind speed has dropped significantly in most regions of the world under global warming [11–13]. Guo et al. reported that the decrease in dust storms in northern China in the 21st century was the result of a decline in wind speed [14]. In this sense, wind regime research is not only an important part of the study of the surface system

but also the essential basis for studying the evolution and distribution of the aeolian sand landform [9,15–17].

Sand drift potential (DP) is the most widely adopted indicator in studying regional sand transport capacity in aeolian sand geomorphology [18,19]. Basically, DP is also known as the sand drift wind energy, which represents the maximum potential sand drift capacity. It is an important parameter in assessing the regional aeolian sand activity intensity and aeolian sand landform evolution [20,21]. DP is also widely used in sand prevention engineering [22,23]. Among the numerous methods developed for DP calculation, Belly [24] experimentally demonstrated that the theoretical curve calculated by adopting the Fryberger and Dean method [25] (adapted from the Lettau and Lettau equation [26]) agreed well with the wind tunnel results. With the wind data of 108 stations in 13 deserts around the world, Fryberger and Dean evaluated the wind energy environment of different deserts and proposed the classification standard of wind energy environment according to the calculated DP value [25]. Due to its simplicity, the Fryberger DP method is widely used internationally. Many studies adopted this method to evaluate the wind energy environment of the Yazd-Ardakan Plain [27], Nile Valley and Delta [28,29], Bermuda [30], Algerian Hautes Plaines [31], Negev Desert of Israel [32], Kuwait [33,34], Rio Grande do Sul coast of southern Brazil [35], northern Denmark [36] and other regions.

In the Alxa Plateau, the Badain Jaran Desert (BJD) is the second biggest mobile desert in China, with the highest sand mounts in the world. It has attracted the attention of many researchers due to its fantastic landscape of coexisting megadunes and lakes. In recent years, some researchers proposed plausible hypotheses on the formation of megadunes [37,38], analyzed the relationship between the dune morphological parameters [39,40] and assessed the wind energy environment in the BJD. According to the wind data of four weather stations around the BJD, Wang et al. (2005) calculated that the DP in the 1990s was 41–371 VU [41]. By installing an automatic meteorological station near Alxa you Qi, Zhang et al. (2013) monitored and reported about an obvious local circulation between the megadunes and lakes in the BJD [42]. Using the wind data of seven weather stations around the BJD in 2001–2011, Zhang et al. (2015) analyzed the spatial variation characteristics of DP and suggested that DP declined from north to south [43]. Regarding the earlier studies on wind regime with short period data, it is necessary to investigate the long-term wind regime evolution and analyze the reasons and consequences of wind speed change. This manuscript describes further analysis on the wind data gathered from eight meteorological stations near the BJD over the past 46 years, the temporal (interannual and seasonal) variation and spatial distribution features of wind speed and DP in the BJD, and a discussion on the association between atmospheric circulation and wind speed. This would enable us to obtain a deeper recognition of the long-term variation characteristics of wind regime in the BJD. The outcome could reveal the characteristics of regional wind energy environment and the pattern of aeolian sand transport and provide a theoretical basis for regional wind energy environment assessment and aeolian sand hazard prevention.

2. Materials and Methods

2.1. Study Area

BJD is the second biggest mobile sand desert in China. It covers an area of about 49,000 km^2 in the center of the Alxa Plateau [44]. Located deeply inland and far away from the ocean, BJD is controlled by the southeast monsoon and Mongolian-Siberian high seasonality [39], forming an extremely arid temperate continental climate. The annual precipitation is low with large interannual and seasonal variations, mainly concentrated in June to August. Spatially, the precipitation declines from the southeast to the northwest, while the spatial variation of potential evaporation is the opposite. The annual and diurnal variations of temperature are huge, with sufficient sunshine and intense evaporation. Northwest and west winds prevail throughout the year. Previous studies have shown that prior to the Last Glacial Period, the main wind direction in the BJD was west wind, followed by northwest wind. Since the Last Interglacial Period, the main wind direction has

changed into northwest wind, followed by west wind, and the prevailing wind direction is still the northwest wind nowadays [45]. The BJD is located where the cold air enters China. Influenced by the Mongolian high pressure, the BJD is affected by strong winds and frequent sandstorms in the spring. In addition, drought and sparse vegetation is a common sight in the desert and the surrounding areas, so it has been one of the major origin places of sandstorms in China.

In geological structure, the main body of the BJD belongs to the depression of the Alxa Plateau at the junction of the north China plate, the Tarim plate and the Xing'an-Mongolian orogenic belt. The BJD lies to the east of the Alluvial Plain of Heihe Downstream and Gulunai Lake, south of Hongshi Mountains, Guaizihu and Malagai Mountains, west of Alateng Mountains, northwest of Yabrai Mountains, north of Heli Mountains and Beida Mountains. The desert is located in a huge basin surrounded by mountains on three sides (Figure 1). Moreover, the altitude gradually declines from the southeast to the northwest. The Yabrai Mountain is the boundary between the BJD and the Tengger Desert. The Heli Mountain and Beida Mountain separate the BJD from the Hexi Corridor [46]. The highest megadunes across the world are distributed in the southeast of the desert, with dune height varying from 200 m to 450 m. Many lowland salt-water lakes are distributed among the dunes [47]. The dune types in the BJD include crescent, transverse, compound transverse and star dunes.

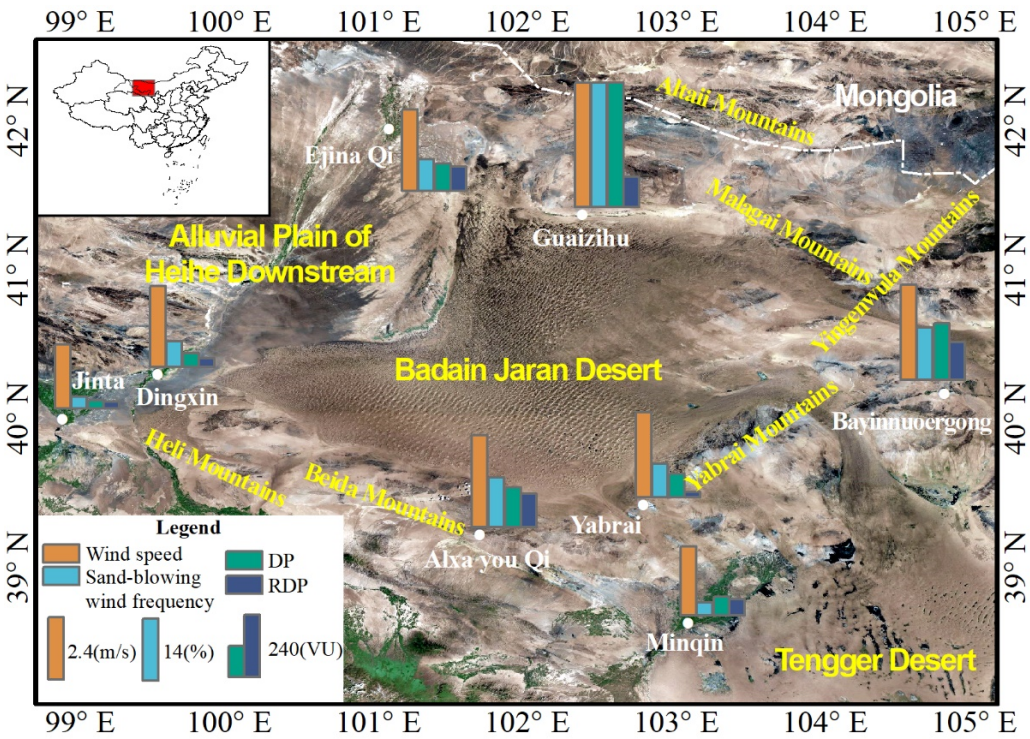

Figure 1. The location of the Badain Jaran Desert (BJD) and wind regime in the BJD. The yellow, blue, green and purple bars represent wind speed, sand-blowing wind frequency, DP and RDP, respectively.

2.2. Data

2.2.1. Meteorological Information

The daily mean wind speed and direction (10 m high) of the eight meteorological stations around the BJD (i.e., Ejina Qi, Guaizihu, Bayinnuoergong, Dingxin, Jinta, Minqin, Alxa you Qi and Yabrai) in 1971–2016 were offered by the China Meteorological Data Network (http://data.cma.cn (accessed on 2 March 2020)). The daily mean wind speed is the mean of the 10 min mean wind speed at 02:00, 8:00, 14:00 and 20:00. The longitude and latitude of each station and the periods of data are shown in Table 1.

Table 1. Elementary information of the eight meteorological stations around the BJD.

Station (ID)	Lat./Lon. (°N/°E)	Elevation (m)	Period of Data
Ejina Qi (52267)	41.95/101.07	940.5	1971–2016
Guaizihu (52378)	41.37/102.37	960	1971–2016
Bayinnuoergong (52495)	40.17/104.8	1323.9	1971–2016
Dingxin (52446)	40.3/99.52	1177.4	1971–2016
Jinta (52447)	40/98.88	1270.5	1971–2016
Minqin (52681)	38.63/103.08	1367.5	1971–2016
Alxa you Qi (52576)	39.22/101.68	1510.1	1971–2016
Yabrai (52575)	39.42/102.78	1239.5	1971–2016

2.2.2. Atmospheric Circulation Indices

The Arctic oscillation (AO) and North Atlantic oscillation (NAO) in 1971–2016 were offered by the NOAA's Climate Prediction Center (https://www.cpc.ncep.noaa.gov/ (accessed on 19 October 2020)). In particular, we gathered the northern hemisphere subtropical high intensity index (NHSHII), the Western Pacific subtropical high intensity index (WPSHII), the Asia polar vortex area index (APVAI), the northern hemisphere polar vortex area index (NHPVAI), the Asian zonal circulation index (AZCT), the Asian meridional circulation index (AMCT), the east Asian trough intensity index (EATII) and the Tibet Plateau Region 2 Index (TPR2I) from the China national climate center's climate system supervision, diagnosis, forecast and assessment system (https://cmdp.ncc-cma.net/cn/download.htm (accessed on 19 October 2020)) [48].

2.3. Methods

2.3.1. Statistical Approaches

This research applied the linear regression approach to analyze the trend of long-term series of wind speed or other factors and used the cumulative anomaly approach [49] to examine whether the wind speed had a mutation. In addition, the significance extent of the association between the various circulation indices and wind speed in various periods was quantified with the correlation analysis approach [50].

2.3.2. Wind Rose

The frequency of sand-blowing winds in 16 directions of each meteorological station was counted, and a wind rose map was plotted. Briefly, a wind rose map can reflect the sand-blowing wind regimes, which provides a basis for the classification of wind direction. There are five common wind regimes [2,20]:

Narrow unimodal wind regimes, i.e., the wind direction frequency of a meteorological station is 90 % or more within two adjacent directions or within 45° arc of the compass;

Wide unimodal wind regimes, i.e., any other direction distribution with a single peak or mode;

Acute bimodal wind regimes, i.e., a distribution with two modes where the peak of the two modes forms an acute angle;

Obtuse bimodal wind regimes, i.e., a distribution with two modes where the peak of the two modes forms an obtuse angle;

Complex wind regimes, i.e., a distribution with more than two modes.

2.3.3. Sand Drift Potential

1. Definition of sand-blowing wind

In aeolian sand physics, the wind speed for the sand to start moving is defined as the threshold wind speed, and the wind speed greater than the threshold wind speed is called the sand-blowing wind. Only the sand-blowing wind can transport surface sand sediment and then shape the aeolian sand landform [2]. Sand-blowing wind frequency is the percent of sand-blowing wind time to total observation time. According to existing research, we set the threshold wind speed as 6 m/s at 10 m above ground [51].

2. Calculation of sand drift potential

DP is a quantitive indicator to measure aeolian sand activity intensity. It represents the potential sand transport capacity and reflects the ability of wind in a certain direction to transport sand in a certain period. DP is calculated by using the wind speed and frequency of the sand-blowing wind [2,18,19]. Typically, the calculation of DP is carried out using the approach proposed by Fryberger and Dean [25]:

$$DP = \sum_{i=1}^{N} V^2 \times (V - V_t) \times t_i, (t_i = 1/N, V > V_t)$$

where DP means the sand drift potential in the vector unit (VU); V and V_t stand for the sand-blowing wind speed and threshold wind speed, respectively, in knots (nmile/h); t_i is the time of the sand-blowing wind, in relative frequency; and N is the total number of wind observation records. Following Equation (1), we calculated the DP for each of the 16 wind directions. Next, we quantified the total DP by adding them together. According to the vectorial resultant rule, the resultant drift potential (RDP) can be obtained, which represents the result of the combined action of sand-blowing wind in all directions and reflects the net sand transport capacity. The direction of RDP is called the resultant drift direction (RDD), which represents the direction of sand transport. Directional variability (RDP/DP) means the proportion of RDP to DP. Notably, a ratio close to 1 indicates a unimodal wind regime with a single main drift direction, while that close to 0 means a bimodal wind regime with various drift directions.

Based on Fryberger and Dean, the wind energy environment can fall into low energy (DP < 200 VU), intermediate energy (200 VU $\leq$ DP $\leq$ 400 VU) and high energy (DP > 400 VU) [25]. Depending on the directional variability, the wind regime can be divided into high directional variability (RDP/DP < 0.3), intermediate directional variability (0.3 $\leq$ RDP/DP $\leq$ 0.8) and low directional variability (RDP/DP > 0.8). High directional variability is usually related to complicated or obtuse bimodal wind regimes, intermediate directional variability generally corresponds to obtuse bimodal or acute bimodal wind regimes, while low directional variability is related to wide unimodal or narrow unimodal wind regimes [20].

3. Results

3.1. Wind Speed

3.1.1. Time Variation Features of Wind Speed

Using the linear regression approach, we determined the variation trend rates of annual and seasonal wind speed in the BJD (Figure 2). The annual mean wind speed in the BJD in 1971–2016 was 3.28 m/s, which trended downward with a trend rate of −0.13 m/(s·10a) ($p < 0.001$). We found that the changes of annual and seasonal wind speed were similar, with a significant decline in the late 1980s, and then gradually increased (with fluctuations) after 2000. In order to determine whether there was a mutation in the annual wind speed during the change process, we calculated the mutation year of annual wind speed in the BJD during 1971–2016 based on the cumulative anomaly approach (Figure 2f). The result shows the annual wind speed in the BJD during 1971–2016 had an obvious mutation in 1987. However, there was no significant mutation around 2000; the increase in wind speed was not obvious.

With 1987 as the border, the variation trend rates of annual wind speed before and after the turning point were −0.41 m/(s·10a) ($p < 0.001$) and 0.12 m/(s·10a) ($p < 0.001$), respectively, while after 2000, the wind speed trended upward, and the trend rate was 0.17 m/(s·10a) ($p < 0.01$). The seasonal wind speeds all showed a downward trend in the BJD during 1971–2016, with the most significant downward trend in the spring and winter; the tendency rates were both −0.14 m/(s·10a) ($p < 0.001$). From 1971 to 1987, the seasonal wind speed trended downward, with the most significant downward trend in the summer, and the tendency rate was −0.53 m/(s·10a) ($p < 0.001$). From 1988 to 2016, the seasonal wind speeds all trended upward, where the most significant upward trend occurred in

the winter, and the trend rate was 0.16 m/(s·10a) ($p < 0.001$). After 2000, the seasonal wind speeds all trended upward, except spring, where the most significant upward trend occurred in the winter, and the trend rate was 0.24 m/(s·10a) ($p < 0.01$). To generalize, the annual and seasonal wind speed all experienced a significant decline in the late 1980s and then gradually increased after 2000; the annual wind speed mutated in 1987, indicating an opposite tendency before and after the turning point.

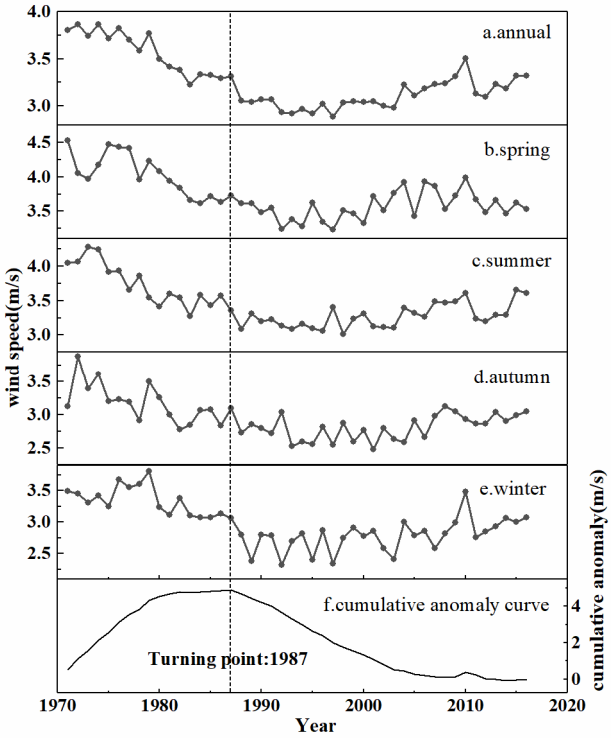

Figure 2. Change process of (**a**) annual, (**b**) spring, (**c**) summer, (**d**) autumn, (**e**) winter wind speed and (**f**) cumulative anomaly curve of annual wind speed in the BJD. The black dots and line indicate the annual and seasonal wind speed during 1971–2016; the black solid line indicates the cumulative anomaly curve of annual wind speed during 1971 to 2016; the black dashed line means the turning point.

The statistical calculation of the daily wind speed above the threshold in the BJD was performed, and the annual mean sand-blowing wind speed and frequency were acquired (Figure 3). The annual mean sand-blowing wind speed and frequency in the BJD in 1971–2016 were 7.13 m/s and 9.71%, respectively. They all exhibited a downward trend, where the variation trend rates were −0.14 m/(s·10a) ($p < 0.001$) and −1.91%/10a ($p < 0.001$), respectively. Based on the cumulative anomaly approach, we calculated the mutation year of the annual sand-blowing wind speed in the BJD during 1971–2016. The results show that the annual sand-blowing wind speed mutated significantly in 1987, which was the same time as the wind speed. Taking 1987 as the boundary, the variation trend rates of the annual sand-blowing wind speed before and after the turning point were −0.24 m/(s·10a) ($p < 0.001$) and −0.02 m/(s·10a). The change tendency rates of the annual sand-blowing wind frequency before and after the turning point were −4.44%/10a ($p < 0.001$) and 0.19%/10a, respectively. The annual sand-blowing wind speed and frequency both had a "cliff-like" drop in the 1980s. After that, the annual sand-blowing wind speed continued to decrease slowly in the fluctuation, and the annual sand-blowing wind frequency increased slightly. To summarize, the annual sand-blowing wind speed and frequency both demonstrated a significant downward trend in the BJD from 1971 to 2016, and both showed a dramatic decline in the 1980s (without obvious upward or downward trend thereafter).

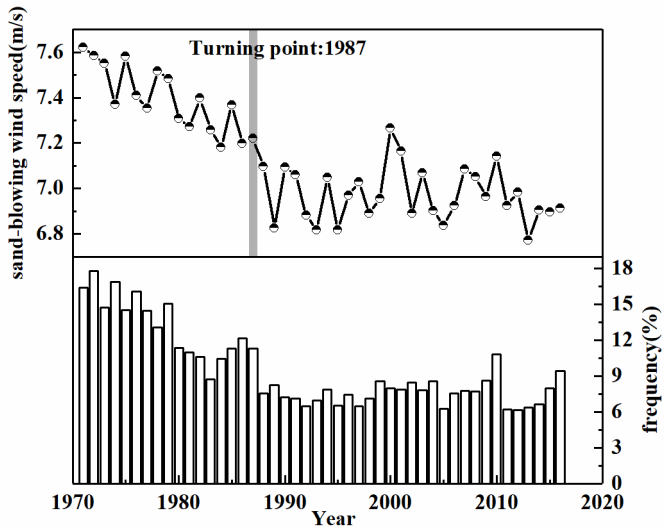

Figure 3. Annual sand-blowing wind speed and frequency in the BJD. The black line indicates annual sand-blowing wind speed during 1971–2016; the bar means the sand-blowing wind frequency.

To better understand the seasonal characteristics of sand-blowing wind speed and frequency, we took 1987 as the border and estimated the seasonal sand-blowing wind speed and frequency in different periods (Table 2).

Table 2. Seasonal sand-blowing wind speed and frequency in different periods in the BJD.

	Sand-Blowing Wind Speed (m/s)			Frequency (%)		
	1971–1987	1988–2016	1971–2016	1971–1987	1988–2016	1971–2016
Spring	7.54	7.12	7.37	18.41	11.35	13.96
Summer	7.26	6.79	7.11	14.17	7.97	10.26
Autumn	7.23	6.87	7.1	9.19	5.06	6.59
Winter	7.44	6.99	7.29	11.32	5.3	7.54

For the whole study period, the seasonal difference in the sand-blowing wind speed was small, ranging between 7.1 m/s in the autumn and 7.37 m/s in the spring. By contrast, the sand-blowing wind frequency varied greatly between the seasons, the frequency reaching as high as 13.96% in the spring, followed by summer; the frequency in the autumn was about 50% of that in the spring. Both wind speed and frequency peaked in the spring, being strongly reflected in the aeolian sand activity. The wind speed and frequency of the sand-blowing wind in different seasons were both higher before than after the mutation. The sand-blowing wind speed dropped the most in the summer, which was 0.47 m/s less than that before the mutation. The sand-blowing wind frequency decreased the most in the winter, which was only 46.82% of that prior to the mutation. From 1971 to 1987, the sand-blowing wind speed and frequency both peaked in the spring and bottomed in the autumn. The frequency of sand-blowing wind hit as high as 18.41% in the spring, and in the autumn, it was about 50% of that in the spring. From 1988 to 2016, the minimum sand-blowing wind speed of 6.79 m/s appeared in the summer, and the sand-blowing wind frequency in the spring was about twice of that in the autumn. In summary, the seasonal variation was small in sand-blowing wind speed but large in frequency in different periods; and sand-blowing wind frequency in the spring was about twice of that in the autumn. Sand-blowing wind speed and frequency both peaked in the spring, being strongly reflected in the aeolian sand activity.

3.1.2. Spatial Variation Features of Wind Speed

Sand-blowing wind speed varied from 6.99 m/s (of Minqin) to 7.57 m/s (of Alxa you Qi), with a small difference of 0.58 m/s. For exploring the spatial distribution features of wind speed in the BJD, we plotted the spatial distribution map of the wind speed and sand-blowing wind frequency at each station.

Affected by the atmospheric circulation, topography, underlying surface and other factors, wind speed was different at each station in the BJD. Figure 1 shows that the spatial differences in wind speed and sand-blowing wind frequency were apparent. The spatial difference in wind speed was larger than that of the sand-blowing wind speed. The mean wind speed of Guaizihu was the largest, with a value of 4.71 m/s, which was 1.09 m/s above that of Bayinnuoergong, while the mean wind speed of Jinta was the smallest, with a value of 2.42 m/s. There was a huge spatial difference in the sand-blowing wind frequency. The sand-blowing wind frequency in Guaizihu reached as high as 27.87%, far beyond that of the other stations; the frequency in Bayinnuoergong and Alxa you Qi was less than 50% of that in Guaizihu; and the frequency in Jinta and Minqin was almost 10 times smaller than that in Guaizihu. To sum up, the spatial difference in the sand-blowing wind speed was not obvious in the BJD; the wind speed and sand-blowing wind frequency of every station were all high-value centers in Guaizihu, Bayinnuoergong and Alxa you Qi and low-value centers in Jinta, Minqin and Dingxin. The overall pattern was "high in the northeast and low in the southwest ".

3.1.3. Influencing Elements of Wind Speed

The BJD in the western part of the Alxa Plateau, located in the marginal zone of the east Asian summer monsoon [52], has a complex atmospheric circulation system. By combining existing research results [11,12,53,54] and its special location, this study selected 10 atmospheric circulation indices (i.e., AO, NAO, NHSHII, WPSHII, APVAI, NHPVAI, AZCT, AMCT, EATII and TPR2I). To identify the circulation driving elements of wind speed variation, the atmospheric circulation indices were correlated with the wind speed in the BJD. With the turning point in 1987 as the border, we extensively discuss the driving mechanisms of wind speed variation in various periods in this section. Figure 4 shows the related coefficient and significance level between wind speed and various atmospheric circulation indices.

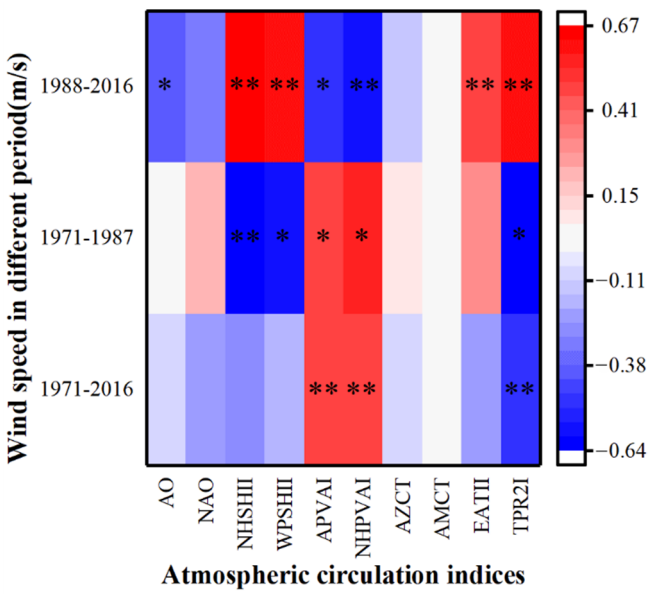

Figure 4. Related coefficient between wind speed and atmospheric circulation indices in different periods in the BJD (* The significance level is 0.05, ** The significance level is 0.01).

For the entire research period (1971–2016), the circulation systems greatly influencing the wind speed variation in the BJD were the Asian polar vortex, the northern hemisphere polar vortex and the Tibet Plateau circulation (Figure 4). The decrease in APVAI and NHPVAI positively influenced the decrease in wind speed (Figure 5d,e), while the increase in TPR2I negatively influenced it (Figure 5g). Taking 1987 as the boundary, the impact of the atmospheric circulation indices on wind speed varied greatly in different periods.

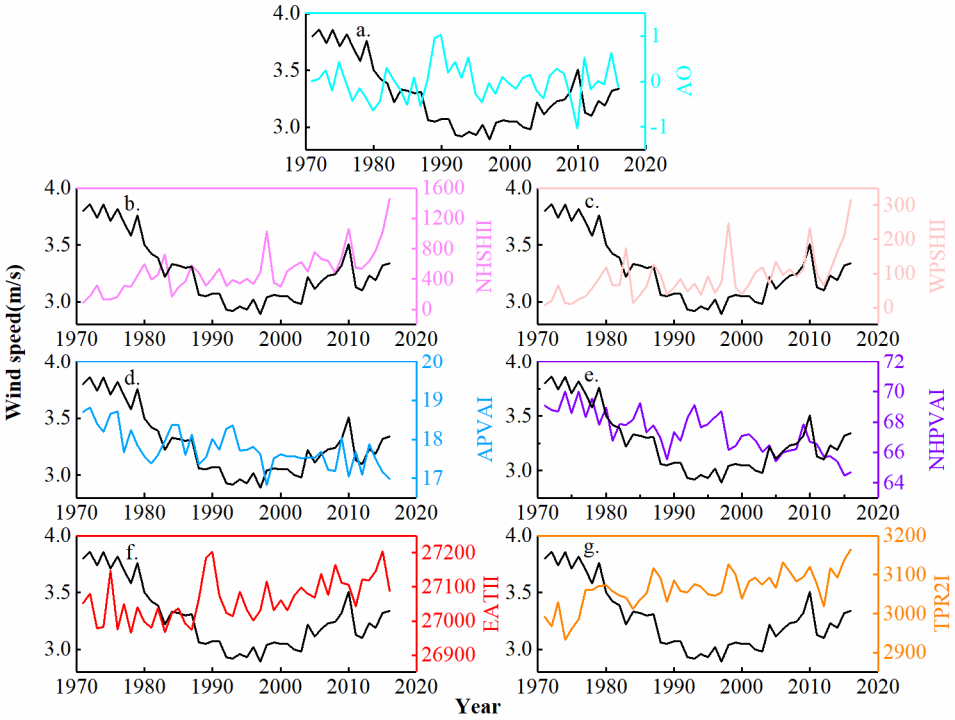

Figure 5. Change process of wind speed and (**a**) AO, (**b**) NHSHII, (**c**) WPSHII, (**d**) APVAI, (**e**) NHPVAI, (**f**) EATII and (**g**) TPR2I in the BJD.

Before 1987, the atmospheric circulation systems greatly influencing the wind speed variation in the BJD included the NHSHII, WPSHII, APVAI, NHPVAI and TPR2I. The APVAI and NHPVAI significantly positively correlated with the wind speed, while the NHSHII, WPSHII and TPR2I significantly negatively correlated with the wind speed. Briefly, the northern hemisphere subtropical high and the Western Pacific subtropical high are both warm high pressures as indispensable members of the east Asian monsoon circulation system, and their changes can influence the climate variation in the east Asian monsoon region [12,55]. During 1971–2016, NHSHII and WPSHII experienced similar trends, and both increased in fluctuations. The subtropical high indirectly affected the wind speed of the BJD by influencing the intensity of the westerly circulation (Figure 5b,c). Apparently, the BJD was also indirectly influenced by the east Asian monsoon. The polar vortex is located in the middle-upper troposphere and stratosphere as a large-scale cyclonic circulation system, and its center is in the polar area. Its activity controls the short-time scale cyclonic activity in the pan-polar region. Changes in the area and intensity of the polar vortex can affect the westerly circulation system and cold air activities [12,56]. The decrease in APVAI and NHPVAI in 1971–2016 indicates the lower polar cold air activity and the weakened westerly circulation intensity, which caused the decrease in near-surface winter monsoon intensity and wind speed in the BJD. A recent study reported that the Tibet Plateau circulation system can affect the near-surface monsoon circulation system and influence the westerly circulation system, which can significantly influence the atmospheric circulation in China and even the world [49]. During 1971–2016, TPR2I experienced an uptrend, and the wind speed in the BJD decreased gradually under the double impact of the monsoon and westerly circulation systems.

After 1987, on top of the five indices mentioned above, the AO and EATII also influenced the wind speed in the BJD. The NHSHII, WPSHII, EATII and TPR2I significantly positively correlated with the wind speed, while the AO, APVAI and NHPVAI significantly negatively correlated with the wind speed (Figure 4). The AO is the biggest and most significant atmospheric circulation pattern in the middle and high latitudes of the northern hemisphere in the winter half year, and it significantly influences the near-surface climatic factors [57,58]. When AO is positive, the strong wind ring around the North Pole will limit cold air across the polar areas; when AO is negative, the weakening of the strong wind ring allows an easier southward penetration of colder air. From 1971 to 2016, in the case of the AO in a positive phase, it mostly corresponded to years with a low wind speed; in the case of the AO in a negative phase, it mostly corresponded to years with a high wind speed. The AO and wind speed were negatively correlated in different periods (Figure 5a). The EAT is a significant circulation system in the middle troposphere over east Asia, and its change can influence the east Asian winter monsoon activity. The EAT is conducive to guiding the cold air in polar and high latitude areas to shift southeast [59,60]. The increase in EATII from 1988 to 2016 indicates that the frequency and intensity of cold air moving southward in high latitudes increased, leading to increased wind speed in the BJD (Figure 5f).

To sum up, atmospheric circulation can significantly alter the wind speed in the BJD. For the whole period of 1971–2016, a combination of the Asian polar vortex, the northern hemisphere polar vortex and the Tibet Plateau circulation affected the wind speed in the BJD. Taking 1987 as the boundary, the influence of the atmospheric circulation indices on the wind speed varied greatly in different periods. From 1971 to 1987, the NHSHII, WPSHII, APVAI, NHPVAI and TPR2I strongly influenced the wind speed change in the BJD. After 1987, in addition to the factors that considerably affected the wind speed before 1987, the AO and EATII also influenced the variation of wind speed in the BJD.

3.2. Wind Direction

The frequency of sand-blowing wind in 16 wind directions at each station in the BJD from 1971 to 2016 was calculated, and the wind roses of sand-blowing wind at each station were drawn in Figure 6.

According to the average situation of each station, the wind rose of sand-blowing wind in the BJD was of the "acute bimodal" type, and the wind direction was relatively single. The majority of wind directions clustered into the W-NW; the main wind direction was WNW, with a frequency of 34.36%. Big diversities were observed in sand-blowing wind direction among the various stations. The wind rose of sand-blowing wind at Ejina Qi, Jinta and Minqin was of the "wide unimodal" type, and the wind direction was relatively consistent, with 79.96–87.5% of sand-blowing wind directions clustered into the W-NW, and the main wind direction was WNW. The wind rose of sand-blowing wind at Alxa you Qi was of the "wide unimodal" type, with 84.25% of sand-blowing wind directions clustered into the ESE-SE. The statistical analysis on the frequency of all winds in 16 wind directions in Alxa you Qi shows that the frequencies of ESE-SE and WNW-NW were 41.31% and 29.18%, respectively. This means that most winds in the WNW-NW did not reach the threshold value.

The wind rose of the sand-blowing wind at Bayinnuoergong was of the "acute bimodal" type, with 68.08% of sand-blowing wind directions clustered into the W-NW, and the main wind direction was WNW with a frequency of 30.02%. The wind rose of the sand-blowing wind at Dingxin was of the "acute bimodal" type, with 62.21% of sand-blowing wind directions clustered into the WSW-WNW, and the main wind direction was WSW with a frequency of 21.26%. The wind rose of the sand-blowing wind at Guaizihu was of the "obtuse bimodal" type; the main and secondary wind directions were W and WNW, respectively, with a total frequency of 49.41%. In addition, the frequency of the E wind was 15.46%, which was the highest among the stations. The Guaizihu station is in the south of the Hongshi Mountain. The blocking effect of mountains on wind is also the reason why the wind direction of Guaizihu is different from the other stations. The wind rose of the

sand-blowing wind at Yabrai was of the "obtuse bimodal" type; the main and secondary wind directions were WNW and ENE, respectively, with 40.79% of the sand-blowing wind directions clustered into the ENE-ESE. The Yabrai station is located in the west of the Yabrai Mountain; the direction of mountains affects the frequency of ENE winds. In summary, the wind rose of the sand-blowing wind in the BJD was of the "acute bimodal" type. The majority of wind directions clustered into the W-NW; the main wind direction was WNW, and the topographic factor was one of the causes of the difference in sand-blowing wind direction between the stations.

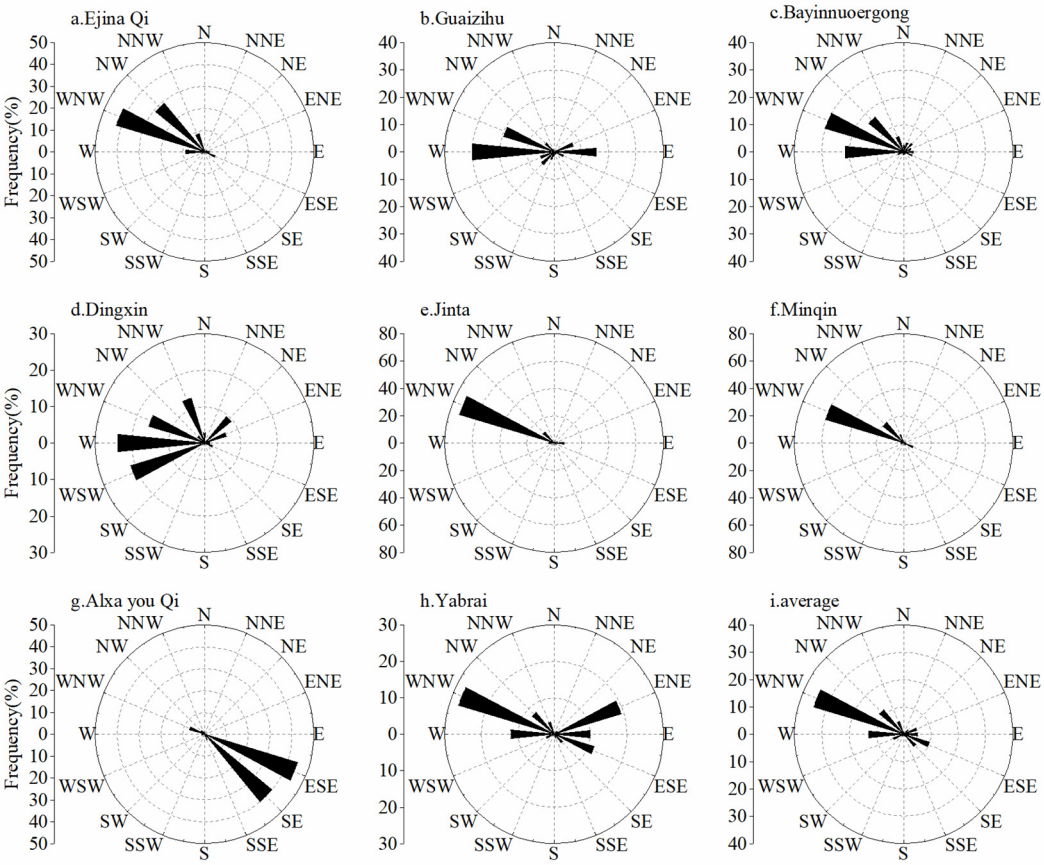

Figure 6. Wind roses of sand-blowing wind at (**a**) Ejina Qi, (**b**) Guaizihu, (**c**) Bayinnuoergong, (**d**) Dingxin, (**e**) Jinta, (**f**) Minqin, (**g**) Alxa you Qi, (**h**) Yabrai and (**i**) BJD.

3.3. Sand Drift Potential

3.3.1. Time Variation Characteristics of Sand Drift Potential

Using the linear regression approach, the variation trend rates of annual DP, RDP and RDP/DP in the BJD were determined (Figure 7).

During 1971–2016, the annual DP, RDP and RDP/DP in the BJD trended downward, and the variation trend rates were −44.69 VU/10a ($p < 0.001$), −44.88 VU/10a ($p < 0.001$) and −0.12/10a ($p < 0.001$), respectively. Taking 1987 as the boundary, the variation trend rates of DP before and after the turning point were −53.99 VU/10a ($p < 0.01$) and −7.69 VU/10a, respectively. The variation trend rates of RDP before and after the turning point were −135.79 VU/10a ($p < 0.001$) and −1.94 VU/10a, respectively. The variation trend rates of RDP/DP before and after the turning point were −0.41/10a ($p < 0.01$) and −0.001/10a, respectively. The annual DP, RDP and RDP/DP dramatically declined in the 1980s and then decreased slowly in fluctuation, but the trend was less obvious.

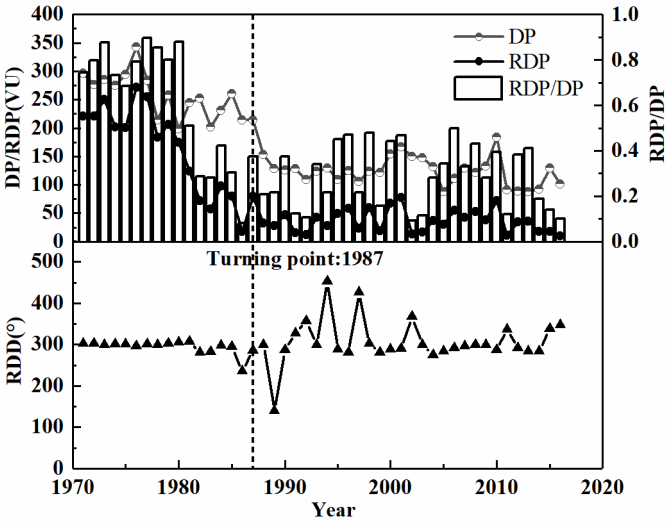

Figure 7. Change process of wind regime (DP, drift potential; RDP, resultant drift potential; RDD, resultant drift direction; RDP/DP, directional variability) before and after the turning point in the BJD.

In contrast, RDD was relatively stable. RDD in 40 years out of 46 years was concentrated in E-SSE, of which 31 years was ESE. RDD was stable in the 1970s; the main direction of sand transport was ESE, and then, RDD varied greatly from the 1980s to the 1990s. RDD in 1986, 1989, 1994 and 1997 were NE, NW, W and WSW, respectively. RDD stabilized after 2000, still being concentrated in ESE, and the frequency of SSE increased significantly after 2010. In short, the annual DP, RDP and RDP/DP in the BJD exhibited a significant downtrend from 1971 to 2016, with a "cliff-like" decline in the 1980s, and then stabilized. RDD was stable and concentrated near ESE.

3.3.2. Spatial Variation Characteristics of Sand Drift Potential

We also calculated the DP, RDP, RDP/DP and RDD of each station in the BJD from 1971 to 2016.

During 1971–2016, the DP of the BJD was 151.38 VU; RDP was 45.12 VU; RDD was toward the ESE (RDD = 296°) in the BJD; RDP/DP was 0.3, which belonged to the intermediate directional variability. The BJD was under a low-energy wind environment with the acute bimodal wind regime. DP was concentrated in W-NW and E-SE, with the highest 42.66 VU in WNW (Figure 8).

The wind energy environment varied widely among the different stations. Among them, Guaizihu was in a high-energy wind environment, with DP of 476.86 VU; Bayinnuoergong was under an intermediate energy wind environment, with DP of 217.19 VU; and other stations were all in a low-energy wind environment. The DP of Jinta was only 31.09 VU, which was the lowest among the stations. The difference in RDP between the stations was not as obvious as that of DP. DP and RDP showed a mode of "high in the northeast and low in the southwest" (Figure 1).

The DPs of Ejina Qi, Bayinnuoergong, Jinta and Minqin were concentrated in W-NW; the RDP/DP were 0.88, 0.68, 0.84 and 0.87, respectively. The RDD was ESE (RDD = 303°, 302°, 295°, 299°). The wind regime of Bayinnuoergong was the acute bimodal wind regime, and the other stations were under the wide unimodal wind regime. Although the RDD of Dingxin was also ESE (RDD = 298°), its DP was concentrated in WSW-NNW, with a wide range of distribution. Its RDP/DP was 0.64, with the acute bimodal wind regime. About 90% of DP at Alxa you Qi was concentrated in ESE and SE. Its RDP/DP was 0.84, and RDD was NW, with the wide unimodal wind regime. Guaizihu and Yabrai were the most complex stations in terms of the wind direction, where both stations had the same RDP/DP of 0.25. The RDDs in Guaizihu and Yabrai were ESE (RDD = 284°) and SE (RDD = 317°), respectively. DP was concentrated in W-NW and ENE-ESE, characterized by the obtuse

bimodal wind regime. In short, the BJD was under a low-energy wind environment with the acute bimodal wind regime. DP was concentrated in W-NW and E-SE, with the highest in WNW. RDD was toward the ESE. DP and RDP exhibited a mode of "high in the northeast and low in the southwest".

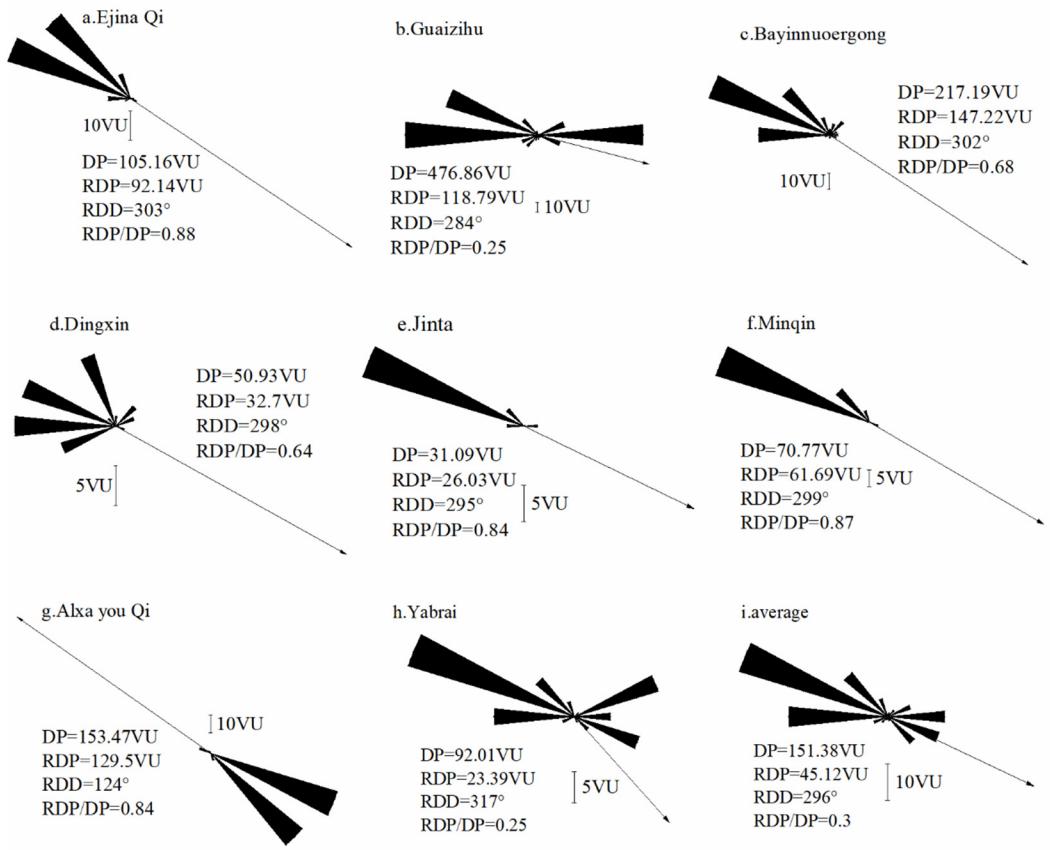

Figure 8. Wind regime of (**a**) Ejina Qi, (**b**) Guaizihu, (**c**) Bayinnuoergong, (**d**) Dingxin, (**e**) Jinta, (**f**) Minqin, (**g**) Alxa you Qi, (**h**) Yabrai and (**i**) BJD.

4. Discussion

In the following section, we will discuss the similarities and differences between the results of previous studies and of this study in terms of the spatial and temporal variations in wind speed and wind energy environment assessment and analyze the possible reasons for the differences.

4.1. Discussion on Wind Speed

In terms of the temporal variation of wind speed, Ma et al. (2011), based on the wind speed data of nine meteorological stations around BJD from 1960 to 2008, concluded that the annual mean wind speed trended downward with a trend rate of −0.09 m/(s·10a), which decreased significantly from the mid-1970s to the mid-1990s, and then increased slightly. The mean wind speed in all seasons decreased, and the most significant trend occurred in the winter, which is basically consistent with the results of this study. However, Ma's study also believed that the winter wind speed had still decreased significantly since 2000. In this study, the seasonal wind speeds all trended upward, except spring, since 2000, with the most significant upward trend occurring in the winter [61]. Zhang et al. (2015) used the hourly wind speeds of seven meteorological stations around the BJD from 2001 to 2011 to calculate the annual mean wind speed of each station; the results obtained were similar to the results of this study. The difference between the two groups of results was within 0.3 m/s, and the mean wind speeds of Guaizihu were all 4.7 m/s [43]. In another study, Zhang et al. (2012) calculated the mean wind speed of seven meteorological stations

around the BJD using the wind data of nearly 40 years before 2012. Although the period of wind data was like this study, Zhang's study did not clearly point out the time precision of wind speed data. The results obtained were quite different from this study, with the mean wind speed of Bayinnuoergong in Zhang's study being about 0.34 m/s less than that of this study. Zhang's study also believed that the wind speed decreased from the northwest to the southeast. The reason for the difference with this study may be that the Zhongquanzi and Toudaohu weather stations were selected in the study, which are located in the southeast of the desert, and Toudaohu is far away from the desert [62]. Yang et al. (2014) established an automatic weather station in the corridor between the BJD and the Tengger Desert and recorded wind data from November 2010 to December 2011 with an interval of 10 min. The monitoring results showed that the annual sand-blowing wind frequency was 16.4%, which mainly occurred in the spring. In this study, the sand-blowing wind frequency was between 2.63% for Jinta and 27.87% for Guaizihu, with an average of 9.71%. The frequency of the sand-blowing wind in the spring was about twice of that in the autumn [51].

4.2. Discussion on Wind Energy Environment

Liu et al. (2010) estimated the DP of the BJD based on the wind data of eight meteorological stations around the desert in the recent 40 years. The result showed that the DP of the BJD has been declining since 1973, and the DP in the late 1990s was about half of that in the early 1970s, which is consistent with this study. The results of RDD and RDP/DP of each station are relatively consistent with this study. In addition, the study also evaluated the wind regime of Zhangye and Shandan in the Hexi Corridor and Alxa Left Banner in the southeast of the desert and far away from it. The results of the Alxa Left Banner were significantly different from other stations; the RDD was W, which may be due to the station being far away from the desert and greatly affected by the east Asian monsoon [39]. Dong et al. (2004) selected the wind data of Ejina Qi, Guaizihu and Dingxin from 1996–2001, 1998–2001 and 1997–2001 to evaluate the wind energy environment in the BJD. The results showed that Guaizihu was under a high-energy wind environment, with a DP of 595 VU. Ejina Qi and Dingxin were both under a low-energy wind environment, with the DP of 81 VU and 63 VU, respectively. The RDP/DP of Guaizihu was 0.29, corresponding to the obtuse bimodal wind regime. Ejina Qi and Dingxin both belonged to the intermediate directional variability, which is consistent with this paper. The RDD of Guaizihu was E (RDD = 275°), while it was ESE (RDD = 284°) in this study, and the RDDs of Ejina Qi and Dingxin were both ESE, which is consistent with the result of this study [37]. Based on the wind data of Ejina Qi, Bayinnuoergong and Dingxin from 1996 to 2001, 1995 to 1998 and 1997 to 2001, Wang et al. (2005) calculated the annual DP of Bayinnuoergong was between 118 VU and 371 VU, with some years reaching a high-energy wind environment. The annual DPs of Ejina Qi and Dingxin were between 44 VU and 116 VU and 41 VU and 70 VU, respectively. This is consistent with the overall pattern of wind energy environment in this study [41].

Since 2010, the study of wind energy environment in the BJD has also added the stations on the southwest and southeast edges of the desert. Yang et al. (2011), based on the wind data of Alxa you Qi, Bayinnuoergong, Dingxin, Ejina Qi and Guaizihu from 1965 to 2004, concluded that Guaizihu and Alxa you Qi were both in a high-energy wind environment; the DP of Guaizihu was as high as 595 VU, which was much higher than that of the other stations. Bayinnuoergong was in an intermediate energy wind environment, Dingxin and Ejina Qi were both in a low-energy wind environment. The results of wind directional variability in Bayinnuoergong, Dingxin, Ejina Qi and Guaizihu were consistent with this study; the RDP/DP in Alxa you Qi was 0.5, indicating variable wind direction, while Alxa you Qi was under a wide unimodal wind regime in this study. There were significant differences in the RDD results between the two group results [38]. Yang et al. (2014) established an automatic weather station on the corridor between the BJD and the Tengger Desert. Based on the 10 min interval wind data in 2011, the DP was calculated to be 729.3 VU, which was much higher than that of Guaizihu (DP = 476 VU), with

the largest wind energy environment in this study. The reason for the large difference may be that the meteorological station is located in the corridor between the two deserts, and the "channeling effect" will lead to a higher wind speed in this area than in other meteorological stations around the desert, and the time interval of the wind data in Yang's study was 10 min, which was easier for capturing the details of the wind speed change, and the frequency of the sand-blowing wind was relatively high [51]. Zhang et al. (2015) selected the wind data from 2001 to 2011 of seven stations in this study, except Minqin. The results showed that Guaizihu and Bayinnuoergong were both in a high-energy wind environment, and the DP of Guaizihu was as high as 733 VU. Alxa you Qi was under an intermediate energy wind environment, and the other stations were all in a low-energy wind environment. In this study, only Guaizihu was in a high-energy wind environment. There was little difference in the RDD between the two groups of results, which was the same or adjacent direction [43].

To sum up, the difference in the period and time precision of the wind data will lead to differences in the results. As for DP, although the values are different, the overall pattern of spatial distribution is similar. RDD is relatively stable in different studies, indicating that the wind direction variation in different time precision data is small, and the wind direction is also relatively stable in the interannual variation; the wind speed is pulsating, and the wind direction is stable.

5. Conclusions

Wind is a key element of the atmospheric circulation. In this paper, we analyzed the temporal and spatial variations of wind speed and DP in the BJD and discussed the association between the atmospheric circulation and wind speed. The results showed that the annual and seasonal wind speeds all experienced a significant decline in the late 1980s and then gradually increased after 2000. The annual wind speed mutated in 1987, showing opposite trends in different periods. The annual sand-blowing wind speed and frequency both demonstrated a significant downtrend and both exhibited a drastic decline in the 1980s.

Atmospheric circulation can considerably influence the wind speed in the BJD, and atmospheric circulation systems can vary greatly in different periods. For instance, before 1987, the decrease in wind speed was the outcome of the integrated action of the NHSHII, WPSHII, APVAI, NHPVAI and TPR2I. Nonetheless, after the turning point, in addition to the factors that significantly affected the wind speed before 1987, the wind speed was also affected by the AO and EATII.

The wind rose of the annual sand-blowing wind in the BJD was of the "acute bimodal" type; most of the annual wind directions clustered into the W-NW, and the main wind direction was WNW. The topographic factor was one of the causes of the diversity in sand-blowing wind direction between the stations.

The annual DP, RDP and RDP/DP in the BJD showed an obvious downtrend from 1971 to 2016, with a "cliff-like" decline in the 1980s, and stabilized thereafter. The DP of the BJD was 151.38 VU; the RDD was toward the ESE. The desert was under a low-energy wind environment with the acute bimodal wind regime. The annual DP was concentrated in W-NW and E-SE, with the highest in WNW. Wind speed, sand-blowing wind frequency and DP of each station were all high-value centers in Guaizihu, Bayinnuoergong and Alxa you Qi and low-value centers in Jinta, Minqin and Dingxin. The overall pattern was "high in the northeast and low in the southwest".

Author Contributions: Conceptualization, Z.H. and L.L.; methodology, Z.H. and G.W.; software, Y.L.; validation, Y.G. and X.H. (Xichen Huang); formal analysis, Y.G. and Q.Z.; investigation, X.W. and X.H. (Xu Han); resources, Q.Z., J.D. and R.L.; data curation, J.D. and R.L.; writing—original draft preparation, Z.H.; writing—review and editing, Z.H. and L.L.; visualization, G.W. and Y.L.; supervision, L.L.; project administration, P.S., G.Z. and J.L.; funding acquisition, L.L. All authors have read and agreed to the published version of the manuscript.

Funding: This research was funded by the National Natural Science Foundation of China, grant number 41730639.

Institutional Review Board Statement: Not applicable.

Informed Consent Statement: Not applicable.

Data Availability Statement: Wind data and atmospheric circulation indices are publicly available from the corresponding web resources cited in the paper.

Acknowledgments: The authors thank the anonymous reviewers and editor who assisted in improving the quality of this paper.

Conflicts of Interest: The authors declare no conflict of interest.

References

1. Mainguet, M. *Desertification: Natural Background and Human Mismanagement*; Springer Science & Business Media: Berlin, Germany, 2012.
2. Wu, Z. *Geomorphology of Wind-Drift Sands and their Controlled Engineering*; Science Press: Beijing, China, 2003.
3. Zhu, Z.D. Concept, cause and control of desertification in China. *Quat. Sci.* **1998**, *2*, 145–155.
4. Liu, L.Y.; Skidmore, E.; Hasi, E.; Wagner, L.; Tatarko, J. Dune sand transport as influenced by wind directions, speed and frequencies in the Ordos Plateau, China. *Geomorphology* **2005**, *67*, 283–297. [CrossRef]
5. Bagnold, R.A. *The Physics of Blown Sand and Desert Dunes*; Courier Corporation: New York, NY, USA, 2012.
6. Cooke, R.U.; Warren, A. *Geomorphology in Deserts*; University of California Press: Berkeley, CA, USA; Los Angeles, CA, USA, 1973.
7. Lancaster, N. *Geomorphology of Desert Dunes*; Routledge: London, UK; New York, NY, USA, 2013.
8. Azorin-Molina, C.; Guijarro, J.A.; McVicar, T.R.; Vicente-Serrano, S.M.; Chen, D.L.; Jerez, S.; Espirito-Santo, F. Trends of daily peak wind gusts in Spain and Portugal, 1961–2014. *J. Geophys. Res.-Atmos.* **2016**, *121*, 1059–1078. [CrossRef]
9. Liu, Z.Y.; Dong, Z.B.; Zhang, Z.C.; Cui, X.J.; Xiao, N. Spatial and temporal variation of the near-surface wind regimes in the Taklimakan Desert, Northwest China. *Theor. Appl. Climatol.* **2019**, *138*, 433–447. [CrossRef]
10. Pryor, S.C.; Barthelmie, R.J.; Schoof, J.T. Inter-annual variability of wind indices across Europe. *Wind. Energy* **2006**, *9*, 27–38. [CrossRef]
11. Song, T.Y. *Variation Characteristics of Wind Velocity and Wind Energy of the Latest 30 Years in China*; Nanjing University of Information Science & Technology: Nanjing, China, 2014.
12. Tian, L. *Studies on Characteristics and Impact Factors of the Surface Wind Speed Changes in the Northern China*; Lanzhou University: Lanzhou, China, 2012.
13. Vautard, R.; Cattiaux, J.; Yiou, P.; Thépaut, J.N.; Ciais, P. Northern hemisphere atmospheric stilling partly attributed to an increase in surface roughness. *Nat. Geosci.* **2010**, *3*, 756–761. [CrossRef]
14. Guo, H.; Xu, M.; Hu, Q. Changes in near-surface wind speed in China: 1969–2005. *Int. J. Climatol.* **2011**, *31*, 349–358. [CrossRef]
15. Zhang, K.C.; Qu, J.J.; An, Z.S. Characteristics of wind-blown sand and near-surface wind regime in the Tengger Desert, China. *Aeolian Res.* **2012**, *6*, 83–88. [CrossRef]
16. Zhang, Z.C.; Dong, Z.B. Research progress on aeolian geomorphology and morphodynamics. *Adv. Earth Sci.* **2014**, *29*, 734–747.
17. Zu, R.P.; Xue, X.; Qiang, M.R.; Yang, B.; Qu, J.J.; Zhang, K.C. Characteristics of near-surface wind regimes in the Taklimakan Desert, China. *Geomorphology* **2008**, *96*, 39–47. [CrossRef]
18. Wasson, R.J.; Hyde, R. A test of granulometric control of desert dune geometry. *Earth Surf. Process. Landf.* **1983**, *8*, 301–312. [CrossRef]
19. Wasson, R.J.; Hyde, R. Factors determining desert dune type. *Nature* **1983**, *304*, 337–339. [CrossRef]
20. Mckee, E.D. *A Study of Global Sand Seas*; U.S. Government Printing Office: Washington, DC, USA, 1979.
21. Pye, K.; Tsoar, H. *Aeolian Sand and Sand Dunes*; Springer: Berlin/Heidelberg, Germany, 2009.
22. Cheng, J.J.; Jiang, F.Q.; Xue, C.X.; Xin, G.W.; Li, K.C.; Yang, Y.H. Characteristics of the disastrous wind-sand environment along railways in the Gobi area of Xinjiang, China. *Atmos. Environ.* **2015**, *102*, 344–354. [CrossRef]
23. Xie, S.B.; Qu, J.J.; Pang, Y.J. Dynamic wind differences in the formation of sand hazards at high-and low-altitude railway sections. *J. Wind Eng. Ind. Aerodyn.* **2017**, *169*, 39–46. [CrossRef]
24. Belly, P.Y. *Sand Movement by Wind (Technical Memorandum)*; U.S. Army Coastal Engineering Research Center: Washington, DC, USA, 1964.
25. Fryberger, S.G.; Dean, G. Dune forms and wind regime. In *A Study of Global Sand Seas*; McKee, E.D., Ed.; US Government Printing Office: Washington, DC, USA, 1979; pp. 137–169.
26. Lettau, K.; Lettau, H.H. Experimental and micrometeorological field studies of dune migration. In *Exploring the World's Driest Climate*; Lettau, H.H., Lettau, K., Eds.; University of Wisconsin-Madison, Institute for Environmental Studies, Center for Climatic Research: Madison, WI, USA, 1978; pp. 110–147.
27. Mesbahzadeh, T.; Ahmadi, H. Investigation of sand drift potential (Case study: Yazd-Ardakan Plain). *J. Agric. Sci. Technol.* **2012**, *14*, 919–928.
28. Hereher, M.E. Assessment of sand drift potential along the Nile Valley and Delta using climatic and satellite data. *Appl. Geogr.* **2014**, *55*, 39–47. [CrossRef]

29. Hereher, M.E. Geomorphology and drift potential of major aeolian sand deposits in Egypt. *Geomorphology* **2018**, *304*, 113–120. [CrossRef]
30. Rowe, M.P.; Bristow, C.S. Landward-advancing Quaternary eolianites of Bermuda. *Aeolian Res.* **2015**, *19*, 235–249. [CrossRef]
31. Louassa, S.; Merzouk, M.; Merzouk, N.K. Sand drift potential in western Algerian Hautes Plaines. *Aeolian Res.* **2018**, *34*, 27–34. [CrossRef]
32. Isenberg, O.; Yizhaq, H.; Tsoar, H.; Wenkart, R.; Karnieli, A.; Kok, J.F.; Katra, I. Megaripple flattening due to strong winds. *Geomorphology* **2011**, *131*, 69–84. [CrossRef]
33. Al-Awadhi, J.M.; Al-Helal, A.; Al-Enezi, A. Sand drift potential in the desert of Kuwait. *J. Arid. Environ.* **2005**, *63*, 425–438. [CrossRef]
34. Al-Enezi, A.; Pye, K.; Misak, R.; Al-Hajral, S. Morphologic characteristics and development of falling dunes, northeast Kuwait. *J. Arid. Environ.* **2008**, *72*, 423–439. [CrossRef]
35. Martinho, C.T.; Hesp, P.A.; Dillenburg, S.R. Morphological and temporal variations of transgressive dunefields of the northern and mid-littoral Rio Grande do Sul coast, Southern Brazil. *Geomorphology* **2010**, *117*, 14–32. [CrossRef]
36. Clemmensen, L.B.; Hansen, K.W.T.; Kroon, A. Storminess variation at Skagen, northern Denmark since AD 1860: Relations to climate change and implications for coastal dunes. *Aeolian Res.* **2014**, *15*, 101–112. [CrossRef]
37. Dong, Z.B.; Wang, T.; Wang, X.M. Geomorphology of the megadunes in the Badain Jaran Desert. *Geomorphology* **2004**, *60*, 191–203. [CrossRef]
38. Yang, X.P.; Scuderi, L.; Liu, T.; Paillou, P.; Li, H.W.; Dong, J.F.; Zhu, B.Q.; Jiang, W.W.; Jochems, A.; Weissmann, G. Formation of the highest sand dunes on Earth. *Geomorphology* **2011**, *135*, 108–116. [CrossRef]
39. Liu, T.; Yang, X.P.; Dong, J.F.; Fan, X.Y.; Li, H.W.; Zhu, B.Q. A preliminary study of relation between megadune shape and wind regime in the Badain Jaran Desert. *J. Desert Res.* **2010**, *30*, 1285–1291.
40. Ning, W.X.; Wang, Z.T. Analysis of morphological parameters of mega-dunes in the southeast of Badain Jaran Desert. *J. Fujian Agric. For. Univ.* **2018**, *47*, 755–763.
41. Wang, X.M.; Dong, Z.B.; Yan, P.; Zhang, J.W.; Qian, G.Q. Wind energy environments and dunefield activity in the Chinese deserts. *Geomorphology* **2005**, *65*, 33–48. [CrossRef]
42. Zhang, K.C.; Ao, Y.H.; Qu, J.J.; An, Z.S. Dynamical environments of wind-blown sand near lakes surrounded by sand-mountains in the Badain Jaran Desert. *Arid Land Geogr.* **2013**, *36*, 790–794.
43. Zhang, Z.C.; Dong, Z.B.; Li, C.X. Wind regime and sand transport in China's Badain Jaran Desert. *Aeolian Res.* **2015**, *17*, 1–13. [CrossRef]
44. Zhu, J.F.; Wang, N.A.; Chen, H.B.; Dong, C.Y.; Zhang, H.A. Study on the Boundary and the Area of Badain Jaran Desert Based on Remote Sensing Imagery. *Prog. Geogr.* **2010**, *29*, 1087–1094.
45. Ma, N.; Wang, N.A.; Li, Z.L.; Chen, X.L.; Zhu, J.F.; Dong, C.Y. Analysis on Climate Change in the Northern and Southern Marginal Zones of the Badain Jaran Desert during the Period 1960–2009. *Arid Zone Res.* **2011**, *28*, 242–250.
46. Zhu, Z.D.; Wu, Z.; Liu, S.; Di, X.M. *Introduction to the Desert in China*; Science Press: Beijing, China, 1980.
47. Yan, M.C.; Wang, G.Q.; Li, B.S.; Dong, G.R. Formation and Growth of High Megadunes in Badain Jaran Desert. *Acta Geogr. Sin.* **2001**, *56*, 83–91.
48. Zhou, J.J.; Huang, J.M.; Zhao, X.; Li, L.; Shi, W.; Wang, L.Y.; Wei, W.; Liu, C.F.; Zhu, G.F.; Yang, X.M. Changes of Extreme Temperature and Its Influencing Factors in Shiyang River Basin, Northwest China. *Atmosphere* **2020**, *11*, 1171. [CrossRef]
49. Zhou, J.J.; Zhao, X.; Wu, J.Y.; Huang, J.M.; Qiu, D.D.; Xue, D.X.; Li, Q.Q.; Liu, C.F.; Wei, W.; Zhang, D.X.; et al. Wind speed changes and influencing factors in inland river basin of monsoon marginal zone. *Ecol. Indic.* **2021**, *130*, 108089. [CrossRef]
50. Li, Z.P.; Gao, X.J.; Lu, D.G. Correlation analysis and statistical assessment of early hydration characteristics and compressive strength for multi-composite cement paste. *Constr. Build. Mater.* **2021**, *310*, 125260. [CrossRef]
51. Yang, Y.Y.; Qu, Z.Q.; Shi, P.J.; Liu, L.Y.; Zhang, G.M.; Tang, Y.; Hu, X.; Lv, Y.L.; Xiong, Y.Y.; Wang, J.P.; et al. Wind regime and sand transport in the corridor between the Badain Jaran and Tengger deserts, central Alxa Plateau, China. *Aeolian Res.* **2014**, *12*, 143–156. [CrossRef]
52. Dong, G.R.; Gao, Q.Z.; Zou, X.Y.; Li, B.S.; Yan, M.C. Climate change in the southern margin of the Badain Jaran Desert since the Late Pleistocene. *Chin. Sci. Bull.* **1995**, *40*, 1214–1218.
53. Duan, C.F. *Study on the Variation of Surface Wind Speed and Its Influencing Factors in China*; Nanjing University of Information Science & Technology: Nanjing, China, 2009.
54. Xing, L.Z.; Zhang, F.M.; Huang, J.; Li, Y.P. Analysis of spatial and temporal change of wind velocity and its affecting factors in Inner Mongolia. *J. Arid Land Resour. Environ.* **2020**, *34*, 162–168.
55. Chen, M.Y.; Yu, J.Y.; Wang, X.; Jiang, W.P. The changing impact mechanisms of a diverse El Niño on the western Pacific subtropical high. *Geophys. Res. Lett.* **2019**, *46*, 953–962. [CrossRef]
56. Woo, S.H.; Kim, B.M.; Kug, J.S. Temperature variation over East Asia during the lifecycle of weak stratospheric polar vortex. *J. Clim.* **2015**, *28*, 5857–5872. [CrossRef]
57. He, S.P.; Gao, Y.Q.; Li, F.; Wang, H.J.; He, Y.C. Impact of Arctic Oscillation on the East Asian climate: A review. *Earth-Sci. Rev.* **2017**, *164*, 48–62. [CrossRef]
58. Rigor, I.G.; Wallace, J.M.; Colony, R.L. Response of sea ice to the Arctic Oscillation. *J. Clim.* **2002**, *15*, 2648–2663. [CrossRef]
59. Song, L.; Wang, L.; Chen, W.; Zhang, Y. Intraseasonal variation of the strength of the East Asian trough and its climatic impacts in boreal winter. *J. Clim.* **2016**, *29*, 2557–2577. [CrossRef]

60. Wang, L.; Chen, W.; Zhou, W.; Huang, R.H. Interannual variations of East Asian trough axis at 500 hPa and its association with the East Asian winter monsoon pathway. *J. Clim.* **2009**, *22*, 600–614. [CrossRef]
61. Ma, N.; Wang, N.A.; Zhu, J.F.; Chen, X.L.; Chen, H.B.; Dong, C.Y. Climate change around the Badain Jaran Desert in recent 50 years. *J. Desert Res.* **2011**, *31*, 1541–1547.
62. Zhang, K.C.; Yao, Z.Y.; An, Z.S.; Xie, S.B. Wind-blown sand environment and precipitation over the Badain Jaran Desert and its adjacent regions. *J. Desert Res.* **2012**, *32*, 1507–1511.